

**The effect of salinity on the wind-driven circulation and
the thermal structure of the upper ocean.**

A.V. Fedorov^{1*}, R. C. Pacanowski², S. G. Philander¹ and G. Boccaletti¹

1. Department of Geosciences, Princeton University, Princeton, NJ

2. Geophysical Fluid Dynamics Laboratory, NOAA, Princeton, NJ

* To whom correspondence should be addressed

E-mail: alexey@princeton.edu

Abstract.

Studies of the effect of a freshening of the surface waters in high latitudes on the oceanic circulation have thus far focused almost entirely on the deep thermohaline circulation and its poleward heat transport. Here we demonstrate, by means of an idealized general circulation model, that a similar freshening can also affect the shallow, wind-driven circulation of the ventilated thermocline and its heat transport from regions of gain (mainly in the upwelling zones of low latitudes) to regions of loss in higher latitudes. A freshening that decreases the surface density gradient between low and high latitudes reduces this poleward heat transport, thus forcing the ocean to gain less heat in order to maintain a balanced heat budget. The result is a deepening of the equatorial thermocline. (The deeper the thermocline in equatorial upwelling zones is, the less heat the ocean gains.) For a sufficiently strong freshwater forcing, the poleward heat transport all but vanishes, and permanent El Niño-like conditions prevail in the tropics. Paleo data indicate that this may have happened before - there was no SST gradient along the equator in the Pacific ocean until approximately three million years ago. The approach to permanent El Niño conditions is shown to introduce a bifurcation mechanism for the north-south asymmetry of the thermal and salinity structure of the upper ocean.

1. Introduction.

The salient feature of the oceanic thermal structure is the remarkably shallow, sharp, tropical thermocline that separates warm surface waters from the cold water at depth. The shallowness of the thermocline is of great importance to the Earth's climate; it permits phenomena such as El Niño which corresponds to a temporary warming of the surface waters of the eastern equatorial Pacific when the zonal slope of the equatorial thermocline decreases. At first it was thought that the maintenance of the shallow thermocline depends mainly on the deep thermohaline circulation, which involves the sinking of cold, saline surface waters in certain high latitude regions. Robinson and Stommel (1959) assumed that the tropical thermocline remains shallow despite the downward diffusion of heat, because that diffusion is countered by the upward motion of cold water from below the thermocline. (The sinking of cold water in high latitudes is a continual source of cold water for the deep ocean.) Subsequently, estimates of the vertical diffusivity k on the basis of measurements (e.g. Ledwell 1993) indicated that in reality the value of k is far smaller than the value required by the theory. This led to a reassessment of the role of the thermohaline circulation in maintaining the oceanic thermal structure.

Today the thermal structure is regarded as depending, not only on the deep thermohaline circulation, but also on the wind-driven circulation of the upper ocean. The latter involves asymmetrical gyres with intense western boundary currents such as the Gulf Stream and Kuroshio Current. The first models of these gyres (Stommel 1948) ignored the vertical structure of the flow. Subsequently Welander (1959), Luyten, Pedlosky and Stommel (1983) and Huang (1988), amongst others, explored the three-dimensional structure of the gyres in the presence of stratification. They introduced

the concept of a ventilated thermocline and identified subtropical regions of "subduction" where the winds force surface water downwards whereafter motion is along surfaces of constant density. Figure 1(a) shows the trajectories of a few sample water parcels over a period of 16 years after subduction in a realistic General Circulation Model of the Pacific Ocean (Harper 2000). Some of the water is seen to join the gyre that includes the Kuroshio Current. Some of the water is seen to flow to low latitudes, ultimately rising back to the surface in the equatorial upwelling zone of the eastern Pacific. The subsequent motion of the water, not shown in fig. 1(a), includes poleward drift in the surface Ekman layer until the water joins the subtropical gyre and ultimately returns to the region of subduction. This circulation, in Ekman layers at the surface, on isopycnal surfaces after subduction, effects a poleward transport of heat, from the equatorial upwelling zone where the ocean gains much of its heat, to higher latitudes where the heat is lost, mainly off Japan. (The regions of gain and loss are shown in fig. 1(b), a map of heat fluxes across the ocean surface.)

The wind-driven ventilated thermocline circulation determines the thermal structure of the upper ocean in the tropics and subtropics. It essentially maps latitudinal temperature gradients onto the vertical. It does so only for the upper ocean because, as is evident in fig. 1(a), the wind-driven circulation penetrates to a depth of a few hundred meters at most. That depth depends on the density of the deep ocean which is maintained by the deep thermohaline circulation. Hence the ventilated thermocline depends on the thermohaline circulation. Theories for the ventilated thermocline (Pedlosky 1996) assume that, in the absence of winds, the depth H of the thermocline is given, and then determine how the winds affect that depth. (Alternatively, in the presence of winds, the depth H is assumed to be known along the eastern boundary of the basin.) This free parameter H in theories for the ventilated thermocline represents the implicit presence of the thermohaline circulation in those theories. What

constraint determines that free parameter? Boccaletti *et al* (2003) propose that a balanced heat budget for the ocean is the relevant constraint. In fig. 1(b) the ocean is seen to gain a very large amount of heat in the equatorial upwelling zone. This would lead to a rapid deepening of the thermocline were it not for the currents that transport the warm water poleward so that the heat is lost in higher latitudes, especially where cold, dry continental air flows over the warm Kuroshio Current (and Gulf Stream in the Atlantic). In a state of equilibrium the gain must equal the loss. Should there be a warming of the atmosphere in mid-latitudes that reduces the oceanic heat loss then warm water accumulates in low latitudes so that the thermocline deepens. The winds then fail to bring cold water to the surface at the equator, the gain of heat is reduced, and a balanced heat budget is restored. This diabatic mechanism whereby surface conditions in higher latitudes can influence the depth of the thermocline in low latitudes on short time scales on the order of decades – those of the wind-driven circulation - is confirmed by scale analyses and numerical experiments with a general circulation model of the ocean (Boccaletti *et al* 2003, Philander and Fedorov 2003). These calculations show that the key factors that determine the thermal structure of the ocean are the heat fluxes across the ocean surface, the winds that drive the ocean, and the diffusivity of the ocean. The latter parameter is of prime importance to the thermal structure at depth, which in turn influences the depth of penetration of the wind-driven circulation.

Both components of the oceanic circulation, the deep thermohaline and the shallow ventilated thermocline circulation, involve meridional overturning – sometimes referred to as conveyor belts – and both contribute to the poleward transport of heat by the oceans. A freshening of the surface waters in high latitudes can inhibit the sinking of cold water and hence can interfere with the conveyor belts and their heat transports. This matter has been studied extensively in connection with the thermo-

haline circulation and it has been established that a sufficiently large freshening in high latitudes can lead to a shut-down of the thermohaline circulation (Manabe and Stouffer 1995, 2000, Rahmstorf 1995, 2000, Stocker and Schmittne 1997, Alley 2003, Seidov and Haupt 2002, 2003). The impact of such a “shut-down” on the Earth’s climate is prominent mainly over the northern Atlantic and western Europe. The reason for a “shut-down” can be inferred from the following reasonably accurate expression for the equation of state that describes the dependence of density ρ on temperature T and on salinity S :

$$\rho = \rho_0(1 - \alpha T + \beta S) \quad (1)$$

where ρ_0 , α and β are constants. An oceanic circulation is possible in the absence of winds provided a density gradient $\Delta\rho$ is imposed at the surface. The maintenance of warm conditions in low latitudes, cold conditions in polar regions drives such a circulation. If density should depend on temperature only, then this circulation disappears when the imposed meridional temperature gradient ΔT vanishes. In the presence of salinity variations, the meridional density gradient, and hence the thermal circulation can disappear even in the presence of a meridional temperature gradient. Equation (1) implies that this happens when

$$\Delta\rho = \rho_0(\alpha\Delta T - \beta\Delta S) \rightarrow 0 \quad \text{or} \quad R \rightarrow 1 \quad \text{where} \quad R = \beta\Delta S / \alpha\Delta T. \quad (2)$$

In the case of the thermohaline circulation the limit $R \rightarrow 1$ is known to be associated with a “breakdown” of that circulation (e.g Zhang *et al* 1999). Such singular behavior occurs because, for the thermohaline circulation, the equator-to-pole density difference $\Delta\rho$ at the surface is also a measure of the vertical density gradient (or the vertical stability of the ocean) in low latitudes. (Note that the plus and minus signs in eq. 2

are chosen for positive $\Delta\rho$, ΔT and ΔS .)

Salinity variations are acknowledged as being of paramount importance to the thermohaline circulation, but their effect on the circulation of the ventilated thermocline has thus far received scant attention. That salinity variations can nonetheless have a major influence on the ventilated thermocline is evident in fig. 2 which shows how temperature and salinity vary on an isopycnal surface on which fluid parcels travel after subduction. In fig. 2(a) temperature variations are as large as 10°C on the $1025\text{kg}/\text{m}^3$ density surface which passes through the core of the Equatorial Undercurrent. Figure 2(b) shows that the warm water is saline, the cold water is relatively fresh, so that the density remains constant. These variations of salinity on the isopycnal surface (on the order of 2-3 psu) reflect salinity variations at the surface where the waters are generally saline in low latitudes (except under the Inter tropical Convergence Zone) and are fresh in high latitudes. How will a further freshening of the extra-tropical waters, especially those near the subduction zone, affect the oceanic circulation and its heat transport? This is the question that this paper addresses.

2. The models and methods.

Studies of the deep thermohaline circulation have to take into account that it is relatively slow, with a time scale on the order of a millennium. Given limited computer resources, investigators choose a relatively coarse spatial resolution to compensate for the demands of simulations of equilibrium states. This paper focuses on the relatively rapid circulation of the ventilated thermocline – time scales are on the order of a decade – so that simulations of equilibrium states require relatively little computer resources. However, spatial resolution has to be high to cope with features such as a

thin thermocline, and narrow equatorial upwelling. To facilitate the study of a large number of cases we configured an idealized version of the oceanic General Circulation Model, known as MOM 4 (Griffies *et al* 2001) to capture the feature of the wind-driven circulation that is most sensitive to variations in surface salinities, namely the meridional overturning involving subduction in higher latitudes, and equatorial upwelling. To this end, the first series of experiments are with a model of modest dimensions -- a rectangular basin of 40° wide, that extends from 16°S to 16°N -- and with high resolution of 0.5° degree in the horizontal and 32 layers in the vertical to a depth of 5000m. The winds that force the model are westward and are spatially uniform of intensity 0.5 dyn/cm^2 .

The vertical diffusion of heat and momentum depends on a Richardson number (Pacanowski and Philander 1981) and has the background vertical diffusion $k=0.01 \text{ cm}^2/\text{s}$. The maximum vertical diffusion reaches $50 \text{ cm}^2/\text{s}$ in the areas of the strong vertical shear associated with the Equatorial Undercurrent. The horizontal diffusion k_h is $0.2 \text{ cm}^2/\text{s}$ in the momentum equations and $0.1 \text{ cm}^2/\text{s}$ in the salinity and heat equations. A linear Rayleigh damping is added at the southern and northern walls to filter out boundary Kelvin waves, but only in the momentum equations. In several sensitivity experiments, instead of using vertical and horizontal diffusivities, we applied an isoneutral mixing, but the results were essentially unaffected.

We use standard mixed boundary conditions on the salt and temperature (e.g. Zhang *et al* 1999):

$$kT_z = A(T^* - T), \quad (3)$$

$$kS_z = (e-p) S_o, \quad (4)$$

where $A=50 \text{ W/m}^2$ is a constant, z is the vertical coordinate, $(e-p)$ is evaporation

minus precipitation and river run-off, S_0 is the mean salinity in the basin, T is the sea surface temperature, and T^* is an imposed temperature. The term $(e-p)$ is parameterized as

$$e-p = B\Phi(\phi) - \Phi_0, \quad (5)$$

where B is a constant, $\Phi(\phi)$ is the latitudinal structure of the forcing (ϕ is latitude), and Φ_0 is a correction such that the overall mean of the forcing is zero. The surface boundary condition is a restoring one for temperature (Haney 1971) but for salinity, equation (4), it is a virtual salt flux through the ocean surface (similar boundary conditions are used in Zhang *et al* 1999, for instance). The use of mixed boundary conditions is related to simple physical arguments: the heat flux depends on evaporation that in turn depends on surface temperatures, but the freshwater flux, to a first approximation, does not depend on the local salinity. The oceanic response can modify the extent to which it is forced thermally, but that is not so in the case of salt. Does this imply that the salinity forcing can reach critical levels that induce marked changes in the response? This is known to be the case in the thermohaline circulation. Is there a similar phenomenon for the wind-driven circulation of the ventilated thermocline?

The latitudinal structure of the forcing is shown in fig. 3, with $T^* = 25^\circ\text{C}$ near the equator and decreasing to 10°C at the northern and southern walls, and $\Phi(\phi)$ equal to 1 at the equator and decreasing linearly to -1 at the walls; Φ_0 is small, but nonzero due to sphericity of the basin; the value of B changes from one experiment to the next. $B=0$ means that there are no salinity variations. This form of the salt flux allows us to simulate the freshening of surface waters in high latitudes without changing the mean salinity of the ocean. Several sensitivity experiments were completed where we

used an explicit freshwater-flux boundary condition instead of the virtual salt flux and prescribed the water flux in the free surface boundary condition. No major differences were found.

At the beginning of a set of calculations, the ocean is at rest, isothermal, and isohaline. After the sudden onset of uniform easterly winds, calculations continue for thirty years in the case of the small ocean basin. By that time the initial adjustment is completed, and the circulation of the ventilated thermocline is in a state of quasi-equilibrium. The deep ocean is still in a state of very gradual adjustment, but this is of secondary importance to the phenomena being investigated here because the oceanic heat budget is close to being balanced with the heat loss in high latitudes nearly equal to the heat gain in low latitudes. The small discrepancy from a balanced heat budget disappears gradually as the deep thermohaline circulation comes into equilibrium. (This strategy of simulations for a relatively short period, a few decades, exploits the considerable difference in the time scales associated with these two circulations - a decade and a millennium respectively, see Boccaletti 2003) In a few additional experiments, described in section 4, the calculations are continued for several centuries to examine possible long-term trends.

The model described above is unrealistic in several respects: the meridional extent of the basin is very modest, an intense western boundary current (Kuroshio or Gulf Stream) is absent (because the winds have no curl), and the regions of subduction are along walls (the poleward ones.) We therefore conducted a second set of experiments, described in section 5, for an ocean basin with a much larger latitudinal and longitudinal extent - that of the Pacific ocean - and with winds with a curl so that the subtropical gyre has an intense western boundary current. The more realistic winds and ocean size do not alter the main results significantly, thus justifying the use of the

smaller basin which requires much less computer resources and is more convenient for conceptual purposes. That the unrealistic features of the first set of experiments are of secondary importance could have been anticipated. For example, the presence of a western boundary current is not necessary for meridional overturning. Furthermore, whether wind-induced subduction occurs along a wall, or where westerly and easterly winds induce Ekman layer convergence, is not of critical importance. Finally, the most important internal latitudinal scale is the radius of deformation – the width of the region of equatorial upwelling for example - which is far smaller than 16 degrees latitude, the latitudinal extent of the small basin.

3. The results for a small ocean basin.

In our reference case the ocean is initially at rest and is isothermal and isohaline, with a temperature of 10°C and salinity of 35psu. After the sudden onset of uniform easterly winds and the thermal forcing of equation (3) - no salinity forcing is applied so that $B = 0$ in equation 5 - calculations continue for 30 years by which time the circulation of the ventilated thermocline is essentially in a state of equilibrium. The meridional thermocline structure of the flow is shown in fig. 4. The model, despite its modest dimensions and simple setting, gives a reasonable representation of the thermocline ventilation and the shallow overturning cell with water parcels sinking along the poleward walls, traveling along isopycnals towards the equator, joining the Equatorial Undercurrent - see fig. 4c - and rising to the surface as part of the equatorial upwelling. Subsequently the flow is poleward in surface Ekman layers (fig. 4b). The slope of the thermocline along the equator, and the sea surface temperature variations will be shown in the top panels of fig. 7. Boccaletti *et al* (2003) describe the effect of changes in T^* (and ΔT) on this motion when no salinity variations are

present. Here we explore the effect of introducing salinity variations.

In the next set of experiments we perturb the ocean conditions by introducing a source of fresh water at the surface near the northern and southern boundaries. To do that, we fix T^* and vary freshwater and salinity fluxes by increasing B - such a procedure increases both the freshwater supply at high latitude and the salt flux at low latitudes so that the mean ocean salinity does not change.

The linear equation of state (equation 1) gives the impression that a decrease in temperature and an increase in salinity affect oceanic conditions similarly. It is already known from the study of Boccaletti *et al* (2003), who neglect salinity variations, that a decrease in the meridional temperature gradient ΔT at the surface causes a decrease in the poleward heat transport. The inclusion of salinity variations alters this result, not only quantitatively as the equation of state would suggest, but also qualitatively, in particular because of the different boundary conditions for temperature and salinity in equations 3 and 4. The results show that, when the freshwater forcing reaches a certain amplitude, the decrease in heat transport suddenly approaches a threshold. This is evident in figs. 5 and 6 which depict how changes in freshwater forcing affect the surface temperature gradient along the equator, the poleward heat transport, the horizontal density ratio R (and hence the value of meridional salinity gradient ΔS - see equation 2), and the depth of the equatorial thermocline. As the fresh water flux near the poleward walls increases from one experiment to the next, the different parameters are seen to change slowly at first and then to change rapidly as R approaches 1.

The slope of the thermocline along the equator, and the sea surface temperature variations for four different values of the fresh-water forcing (indicated as 1, 2, 3 and 4 in

fig. 5) are displayed in fig. 7. The top row of panels of this figure shows the thermocline slope and SST of the reference solution (case 1) with no salinity variations imposed. The second row of panels shows the thermal structure for a relatively weak salinity forcing – the solution is still dominated by temperature and salinity variations have little effect on either thermocline or SST. A further freshening of the surface waters near the northern and southern boundaries, and the associated reduction in the meridional density gradient at the surface, deepens the equatorial thermocline (also fig. 6) and reduces both the size of the equatorial cold tongue and the oceanic heat gain in low latitudes (the third and fourth rows in fig. 7). The corresponding changes in spatial structures in salinity (in the equatorial plane) and density (along a meridian and in the equatorial plane) are shown in figs. 8 and 9, respectively.

When $R > 1$ (the red dots in figs. 5 and 6, and the bottom panels in fig. 7), the thermocline slope in the equatorial plane collapses, the cold equatorial tongue at the surface virtually disappears, and permanent El Niño conditions prevail in the tropics. The collapse of the thermocline eliminates the confined equatorial region where the ocean gains a large amount of heat. As a result, the constraint of a balanced heat budget is no longer satisfied by transporting heat from regions of gain to regions of loss. Rather, the heat budget tends to be balanced locally almost everywhere. (A local balance can be simulated by means of a one-dimensional mixed layer model that takes into account only vertical variations in density). Apparently such a state of affairs can be induced merely by freshening the surface waters in the extra-tropics. In these experiments the winds have remained unchanged so that a zonal pressure gradient along the equator is still needed to balance the winds. With the collapse of the thermocline, that density gradient depends mainly on salinity. The surface water of the eastern Pacific, instead of being cold, is saline, as shown in the bottom panel of fig. 8

Given how abruptly the equatorial thermocline can collapse in fig. 5, it is important to estimate how far oceanic conditions today are from singular behavior near $R=1$. Our results, for a small idealized model of the ocean, need to be rescaled to be appropriate for the much larger Pacific. This difficulty can be sidestepped by focusing on the non-dimensional parameter R . Its value today, approximately 0.5, is indicated by a blue dot in figs. 5 and 6. The results imply that climatic conditions today - high latitudes with heavy rains and river run-off that freshen the surface waters and hence counter the effect of the decrease in temperature with increasing latitude - may put us in a parameter range of relatively high sensitivity to changes in surface buoyancy. Relatively modest changes in the freshening of surface waters (because of the melting of ice or intensification of the global hydrological cycle) may result in a transition to permanent El Niño conditions. Because of the nonlinearity of the equation of state of water and complicated geometry of the ocean, $R=0.5$ is given here as only a very rough estimate. In fact, any value of R between 0.3 and 1 would put the conditions of today on the steep slope in figs. 5 and 6.

The equatorial thermocline collapses when the flux of fresh water onto the surface in extratropical regions is such that the meridional density gradient at the surface vanishes. The cold, fresh surface water near the northern and southern walls then has such a low density that the wind-driven warm, saline water drifting poleward in the Ekman layer subducts beneath the surface water before reaching the northern and southern walls. This can be seen, for instance, from the plots of the meridional streamfunction (not shown here). The subduction of surface water relatively far from the northern or southern wall decreases the loss of heat to the atmosphere, causing a reduction in the heat gained near the equator by means of a deepening of the equatorial thermocline. Salinity gradients along the equator now balance the wind-stress. The thermal structure presumably continues to change because of diffusive processes

with a long time-scale. To investigate such changes we continued some of the simulations for several centuries (see section 4).

Another set of numerical experiments was conducted to investigate the effect of changing meridional temperature gradient ΔT . Boccaletti *et al* (2003) investigated this problem in the absence of salinity and showed that a gradual reduction of ΔT leads to a gradual deepening of the equatorial thermocline. Adding salinity introduces a new phenomenon - the possibility of a rapid thermocline collapse that can be induced solely by changing ΔT . This is because the condition of thermocline collapse $R=0$ (eq.2) can be satisfied either by increasing ΔS (as in fig. 5-6), or by decreasing ΔT , provided that ΔS is nonzero. Our numerical results do indeed show that it is possible to force such thermocline collapse by changing ΔT (when ΔS is fixed).

4. Long-term trends.

The results shown thus far are for calculations that continue for a few decades at most. In a few cases the calculations were continued for 500 years. For zero or weak freshwater forcing the results remained essentially unchanged. For the cases with relatively strong freshwater forcing the lenses of cold, fresh surface water near the northern and southern walls persist (fig. 10) while the deep ocean continues to warm very gradually. The processes involved will apparently take far longer than 500 years to reach equilibrium. The ultimate stratification of the deep ocean is a matter beyond the scope of this paper and will be investigated on another occasion.

On a time-scale of a few centuries, another intriguing phenomenon became apparent, one associated with a bifurcation of possible states (for the cases with no thermocline

collapse). Although the equations being solved, and the initial and the boundary conditions are all symmetrical about the equator, on several occasions the flow over the course of a few centuries acquired asymmetries relative to the equator. This is evident, for example, in fig. 11 which corresponds to case 3 after 500 years. The thermal and salinity structure shows that water in the Southern Hemisphere is warmer and saltier than that in the Northern hemisphere. A sharp boundary between relatively fresh and relatively salty waters appears along the equator. A tongue of cold and fresh water emanates from the subduction region in the north. These asymmetries relative to the equator are in response to extremely small asymmetries introduced by the numerical code. (Presumably, slightly different numerical noise can favor asymmetry that is the mirror image of the one in fig. 11.) This means that the mean state seen in fig. 4, when perturbed slightly, can drift into different possible states. A similar phenomenon - both symmetric and asymmetric equilibrium states - has been long known to be possible for the thermohaline circulation (e.g. Huang *et al* 1992), but here we have shown that a weak bifurcation may also occur for the wind-driven circulation. Significantly, this effect was observed only in the vicinity of $R=1$ (case 2 did not reveal this type of bifurcation).

The thermal and salinity structures in fig. 11 strongly resemble the actual distribution of temperature and salinity in the Pacific ocean (fig. 12). This observed asymmetry is strongly influenced by the asymmetrical surface forcing: it rains more in the Northern than Southern Hemisphere because the Intertropical Convergence Zone (ITCZ) is mostly north of the equator. The results in fig. 11 suggest another factor that could contribute to the observed asymmetry, namely the tendency of a symmetric mean state to drift to an asymmetric state as in fig. 11.

5. The results for a large basin.

The numerical experiments described thus far are for an ocean basin of modest dimensions, forced with winds without any curl. We next increase both the latitudinal and longitudinal extent of the basin, to $48^{\circ}\text{N} - 48^{\circ}\text{S}$ and $120^{\circ}\text{E} - 80^{\circ}\text{W}$, respectively, and impose winds that generate a western boundary current. (We use an analytic approximation to the zonally-averaged annual mean winds by Hellerman and Rosenstein, 1983.) The imposed temperature T^* and the latitudinal structure of the salinity/freshwater forcing $\Phi(\phi)$ are shown in fig. 13. Because of these changes, the regions where the ocean loses heat and where surface water subducts, no longer coincide.

The zonally-integrated meridional structure of the flow is given in fig. 14, which shows the strong tropical overturning cells associated with the thermocline ventilation. It is the similarity of the tropical circulation in fig. 14 and fig 4. (the middle panel) that justifies our use of a small basin in the previous sections.

As in the cases described for a small basin, the thermocline still deepens and the size of the equatorial cold tongue still shrinks as the flux of fresh water onto the surface in high latitudes increases. This is evident in fig. 15 which also shows, in the bottom panel, that for a sufficiently strong freshwater forcing the thermocline collapses. These aspects persist even though, in fig. 16, a map of fluxes across the ocean surface, the strongest heat loss is seen to occur in the region where the western boundary current crosses the isotherms; the maximum heat gain is still in the region of the equatorial cold tongue. When the thermocline collapses and the cold tongue virtually disappears, the heat transport from the equatorial region is significantly reduced. A much broader area of heat gain is now needed to compensate for the heat loss in high

latitudes.

6. Conclusions.

The results described in this paper show that the effects of a flux of fresh water onto the ocean surface in high latitudes on the deep thermohaline circulation, and on the shallow wind-driven circulation of the ventilated thermocline, have certain similarities. A decrease in the meridional density gradient at the surface reduces the poleward heat transport of the circulation in both cases, sharply so when the density gradient approaches zero. Both cases allow the possibility of a bifurcation of the circulation, from a state of symmetric (with respect to the equator) to an asymmetric state, when the fresh water forcing in high latitudes is large enough. The changes in climate because of a sharply reduced poleward heat transport are strikingly different in the two cases. A much weaker thermohaline circulation affects climate conditions primarily in the northern Atlantic; a wind-driven circulation that fails to transport heat poleward is associated with a tendency towards a deep thermocline all along the equator, and permanent El Niño conditions. Since the processes involving the circulation of the ventilated thermocline can occur relatively fast, on the order of a few decades, the transition to perennial El Niño conditions can occur rapidly, given fresh water forcing of sufficiently large amplitude.

The consequences of a freshening of the surface waters in high latitudes depend critically on whether the thermohaline or wind-driven circulation is affected most. In the one case the associated climate changes are prominent in low latitudes where there is a tendency towards permanent El Niño conditions. In the other case the climate changes are prominent in high latitudes. What are the factors that determine which of

these two components of the oceanic circulation is affected most by a freshening? One likely factor is the degree to which a component contributes to the poleward heat transport. In the Pacific Ocean the wind-driven circulation is the main contributor to the heat transport so that a freshening of the surface waters in the high latitudes of that ocean should have a strong effect on conditions in low latitudes. The Atlantic is a far more complicated matter because there the thermohaline circulation too transports a large amount of heat northward. What are the factors that determine whether a freshening of the waters of the northern Atlantic results in a colder climate for northwestern Europe (in accord with results from studies of the thermohaline circulation), or a deeper equatorial thermocline (in accord with the results presented in this paper)? At this time an answer is unavailable; further theoretical studies are necessary but of even greatest importance are observations of past climate changes to check the validity of the theories. There appears to be persuasive evidence that a freshening of the northern Atlantic has been associated with a cooling of northwestern Europe, on occasions such as the Younger Dryas some 12,000 years ago (Broecker 2003). Evidence that our planet experienced permanent El Niño conditions in the past, and that those conditions were associated with a decrease in the meridional density gradient at the surface, are available in geological records that describe the climate changes that occurred some 3 million years ago. El Niño was a permanent phenomenon up to approximately 3 million years ago whereafter cold surface waters started appearing in the oceanic upwelling zones of the eastern equatorial Pacific (Canariato and Ravelo 1997, Chaisson and Ravelo 2000, Ravelo *et al* 2001), off southwestern Africa (Marlowe *et al* 2000) and off California (Ravelo *et al* 2001). The description of Haug *et al* (1999) of a sharp change in the oceanic vertical stratification in the northern Pacific approximately 3 million years ago, is also of considerable interest. For a discussion of these matters see Philander and Fedorov (2003) and Fedorov and Philander (2003).

Whether a freshening of the surface waters in the northern Atlantic will affect mainly the thermohaline or the ventilated thermocline circulation is a matter that remains to be investigated. Further calculations are also needed to investigate the effect of coupled interactions between the ocean and atmosphere. Those interactions, in which a deepening of the thermocline leads to higher equatorial surface temperature gradients and weaker zonal winds (e.g. Dijkstra and Neelin 1995, Fedorov and Philander 2001), could accelerate the tendency towards permanent El Niño conditions. In addition, calculations are needed to explore the links between the wind-driven and thermohaline circulations, the links between those circulations and the Antarctic Circumpolar Current (Toggweiler and Samuels 1998, Gnanadesikan 1999), and a host of other issues. As in the case of the results presented here, the goal should be not only realistic simulations of oceanic conditions at different times in the past or future, but especially the exploration of a broad range of possibilities not previously considered.

References

Alley, R. *et al*: Abrupt Climate Change. *Science* **299**, 2005-2010, 2003

Boccaletti, G., R. C. Pacanowski, S.G. Philander and A. V. Fedorov: The Thermal Structure of the upper ocean. Submitted, *J. Phys. Oceanogr.*, 2003

Boccaletti G. 2003: Timescales and Dynamics of the formation of a thermocline. Submitted, *J. Phys. Oceanogr.*, 2003

Broecker, W. *Science* (2003)

Cannariato, K. G. and Ravelo, A. C. Pliocene-Pleistocene evolution of eastern tropical Pacific surface water circulation and thermocline depth. *Paleoceanogr.* **12**, 805-820 (1997).

Chaisson W.P. and A.C. Ravelo: Pliocene development of the east-west hydrographic gradient in the equatorial Pacific. *Paleoceanogr.* **15**, 497-505, 2000.

Dijkstra H.A. and J.D. Neelin Ocean-atmosphere interactions in the tropical climatology *J. Climate.* **8**, 1343-1359, 1995.

Gnanadesikan, A., 1999: A simple predictive model for the structure of the oceanic pycnocline. *Science* **283**, 2077-2079.

Griffies,S., Harrison,M., Pacanowski,R. and A. Rosati 2001: A Technical Guide to MOM 4: http://www.gfdl.gov/~lat/fms_public_release/public_manual_fms/mom4_manual.html

Fedorov, A.V. and Philander, S.G.H.: Is El Niño changing? *Science* **288**, 1997-2002, 2000.

Harper S.: Thermocline ventilation and pathways of tropical - subtropical water mass exchange. *Tellus* **52A**, 330-345, 2000.

Hellerman, S., and M. Rosenstein, 1983: Normal monthly wind stress over the world ocean with error estimates. *J.Phys. Oceanogr.* **13**, 1093-1104.

Haney, R.L 1971: Surface boundary conditions for ocean circulation models. *J Phys. Oceanogr.* **1**, 241-248

Haug, G. H., D. M. Sigman, R. Tiedemann, T. F.Pedersens, M Sarnthein: Onset of permanent stratification in the subarctic Pacific Ocean. *Nature* **401**, 779-782 , 1999.

Huang, R.X. An analytical solution of the ideal-fluid thermocline. *J. Phys. Oceanogr.* **31**, 2441-2457, 2001.

Huang, R. X.: Solutions of the ideal fluid thermocline with continuous stratification. *J. Phys. Oceanogr.* **16**, 39-59 (1988).

Huang R.X., Luyten J.R. and H. M. Stommel, Multiple equilibrium states in combined thermal and saline circulation. *J. Phys. Oceanogr.* **22**, 231-246 (1992)

Kennet J., G. Keller and M. Srinivasan: Miocene planktonic foraminiferal biogeography and paleoceanographic development of the Indo-Pacific region. In the Miocene Ocean , *Mem. Geol. Soc. Amer.* **163**, 197-236, 1985.

Ledwell, J. R., A. J. Watson, and C. Law, 1993. Evidence for Slow Mixing across the Pycnocline from an Open-Ocean Tracer-Release Experiment. *Nature* **364**, 701-703.

Luyten J.R., J.Pedlosky and H.M. Stommel: The ventilated thermocline *J. Phys. Oceanogr.* **13**, 292-309, 1983.

Marotzke, J., and J. Willebrand: Multiple Equilibria of the global thermohaline circulation. *J. Phys. Oceanogr.* **21**, 1372--1385, 1991.

Manabe, S., Stouffer, R.J.: Study of abrupt climate change by a coupled ocean-atmosphere model. *Quaternary Science Reviews* **19**, 285-299, 2000.

Manabe, S., and R. J. Stouffer: Simulation of abrupt climate change induced by freshwater input to the North Atlantic Ocean. *Nature* **378**, 165-167, 1995.

Molnar, P. and M. Cane: El Niño's tropical climate and teleconnections as a blueprint for pre-Ice Age climates. *Paleoceanogr.* **17**, 2002.

Marlow, J.R., C.B.Lange, G. Wefer, A.Rosell-Mele: Upwelling Intensification as part of the Pliocene-Pleistocene climate transition. *Science* **290**, 2288-2294, 2000.

Pacanowski, R.C. and S.G.Philander: Parameterization of vertical mixing in numeri-

cal-models of tropical oceans *J. Phys. Oceanogr.* **11**, 1443-1451, 1981.

Philander, S. G., and A. V. Fedorov, Role of tropics in changing the response to Milankovich forcing some three million years ago, *Paleoceanography* **18**(2), 1045, doi:10.1029/2002PA000837, 2003.

Pedlosky, J. *Ocean Circulation Theory*. 453pp, Springer Verlag, Heidelberg, 1996.

Ravelo, A. C., D. H. Andreasen, M. W. Wara, M. Lyle, and A. Olivarez:
California margin (Tanner Basin) records of Plio-Pleistocene circulation and climate,
Abstract from Fall meeting of the AGU, 2001.

Rahmstorf, S.: Bifurcation of the Atlantic thermohaline circulation in response to changes in the hydrological cycle. *Nature* **378**, 145-149, 1995.

Rahmstorf, S.: The thermohaline ocean circulation: A system with dangerous thresholds? *Climatic Change* **46**, 247-256, 2000.

Stocker, T.F. and A. Schmittner: Influence of CO₂ emission rates on the stability of the thermohaline circulation *Nature* **288**, 862-865, 1997.

Seidov, D., and B.J. Haupt: On sensitivity of ocean circulation to sea surface salinity, *Global and Planetary Change* **36**, 99-116, 2003.

Seidov, D. and B. J. Haupt, On the role of inter-basin surface salinity contrasts in global ocean circulation. *Geoph. Research Lett.* **29**, 10.1029/2002GL014813.

Stommel, H. M. The western intensification of wind-driven ocean currents. *Trans. Amer. Geophys. Union* **29**, 202-206, 1948.

Stommel, H. M.: Thermohaline convection with two stable regimes of flow. *Tellus* **13**, 224-230, 1961.

Toggweiler, J. R., and B. Samuels, 1998: On the ocean's large-scale circulation near the limit of no vertical mixing. *J Phys. Oceanogr.* **28**, 1832-1852.

Welander, P.: An advective Model of the Ocean Thermocline. *Tellus* **11**, 310-318 (1959)

Zachos, J., M. Pagani, L. Sloan, E. Thomas, K. Billups: Trends, Rhythms, and Aberrations in Global Climate 65 Ma to Present *Science* **292**, 686-693, 2001.

Zhang, J., R.W.Schmitt, R.X.Huang: The relative influence of diapycnal mixing and hydrologic forcing on the stability of the thermohaline circulation. *J. Phys. Oceanogr.* **29**, 1096-1108, 1999.

Legends for figures

Fig. 1. (a) The wind-driven circulation of the Pacific as portrayed in the paths of sample water parcels over a period of 16 years after subduction off the coasts of California and Chile. The trajectories are from a realistic general circulation model of the ocean forced with the observed climatological winds (Happer 2000). The dots, at intervals of one month, indicate rapid motion in the Equatorial Undercurrent and Kuroshio. The colors show the depth of the water parcels which move on the constant density surface in fig 2. (b) The heat flux into the ocean in low latitudes, and out of the ocean in higher latitudes.

Fig. 2. Temperature (a) and salinity (b) variations on the 1025 kg/m^3 density surface in the Pacific ocean.

Fig. 3. The meridional structure of the forcing used in the small-basin calculations - T^* and $\Phi(\phi)$.

Fig. 4. A typical meridional section of the model solutions with no salinity forcing: (a) the thermal structure at the middle of the basin, (b) the zonally-integrated stream function (note the shallow overturning circulation connecting the tropics and extratropics), and (c) the zonal velocity field showing the equatorial undercurrent.

Fig. 5. Changes in (a) the equatorial east-west surface temperature gradient, (b) the meridional heat transport across a fixed latitude and (c) the density ratio R , as the flux of fresh water onto the surface near the northern boundary of the basin increases.

The value of R today, indicated by a blue dot, is such that current conditions are sensitive to relatively modest changes in the warming or freshening of surface waters in higher latitudes. The red dots correspond to cases with $R > 1$. Numbers 1,2,3,4 correspond to cases shown in figs. 7-9. The values of the freshwater flux are calculated by averaging $(e-p)$ over the region where it is positive and re-scaling it to a realistic-size basin.

Fig. 6. Changes in the mean depth of the equatorial thermocline as the flux of fresh water increases. The blue dot indicates current conditions. The red dots correspond to cases with $R > 1$.

Fig. 7. The thermal structure of numerical solutions in the equatorial plane (the left-side column) and the corresponding sea surface temperatures (the right-side column). Notice the collapse of the thermocline in the bottom panels. The freshwater forcing increases from top to bottom.

Fig. 8. The salinity structure of the numerical solutions in the equatorial plane. There are no salinity variations in the upper panel. Note the west-to-east redistribution of salt after the thermocline collapse. The freshwater forcing increases from top to bottom.

Fig. 9. The density structure of the numerical solutions in the equatorial plane (the left-side column) and along a middle meridian (the right-side column). The freshwater forcing increases from top to bottom.

Fig. 10. The details of the meridional structure of numerical solutions after 500 years of integration (for case 4 of figs. 5-9). The equatorial pycnocline is controlled mostly

by salinity variations.

Fig. 11. The details of meridional structure of the numerical solutions after 500 years of integration (case 3 of figs. 5-9). A north-south asymmetry in the thermal and salinity structure has developed. The structure of the solution along the equatorial plane changed only slightly as compare to that shown in fig. 3 (the third left-side panel).

Fig. 12. Meridional (a) temperature and (b) salinity variations along 165°W in the Pacific ocean (c.f. fig. 11).

Fig. 13. The meridional structure of the forcing used in the large-basin calculations - T^* and $\Phi(\phi)$.

Fig. 14. The zonally-integrated stream function in the large-basin calculations with no freshwater forcing. Note the strong overturning circulation connecting the tropics and extra-tropics (c.f. fig. 4, middle panel).

Fig. 15. The thermal structure of numerical solutions in the equatorial plane (the left-side column) and the corresponding sea surface temperatures (the right-side column) - the large-basin calculations. Notice the collapse of the thermocline in the bottom panels. The freshwater forcing increases from top to bottom.

Fig. 16. The downward heat flux (in W/m^2) into the ocean for the solutions shown in the previous figure. Note the different color scales and qualitative similarities with the observed heat flux into the ocean shown in fig. 1(b).

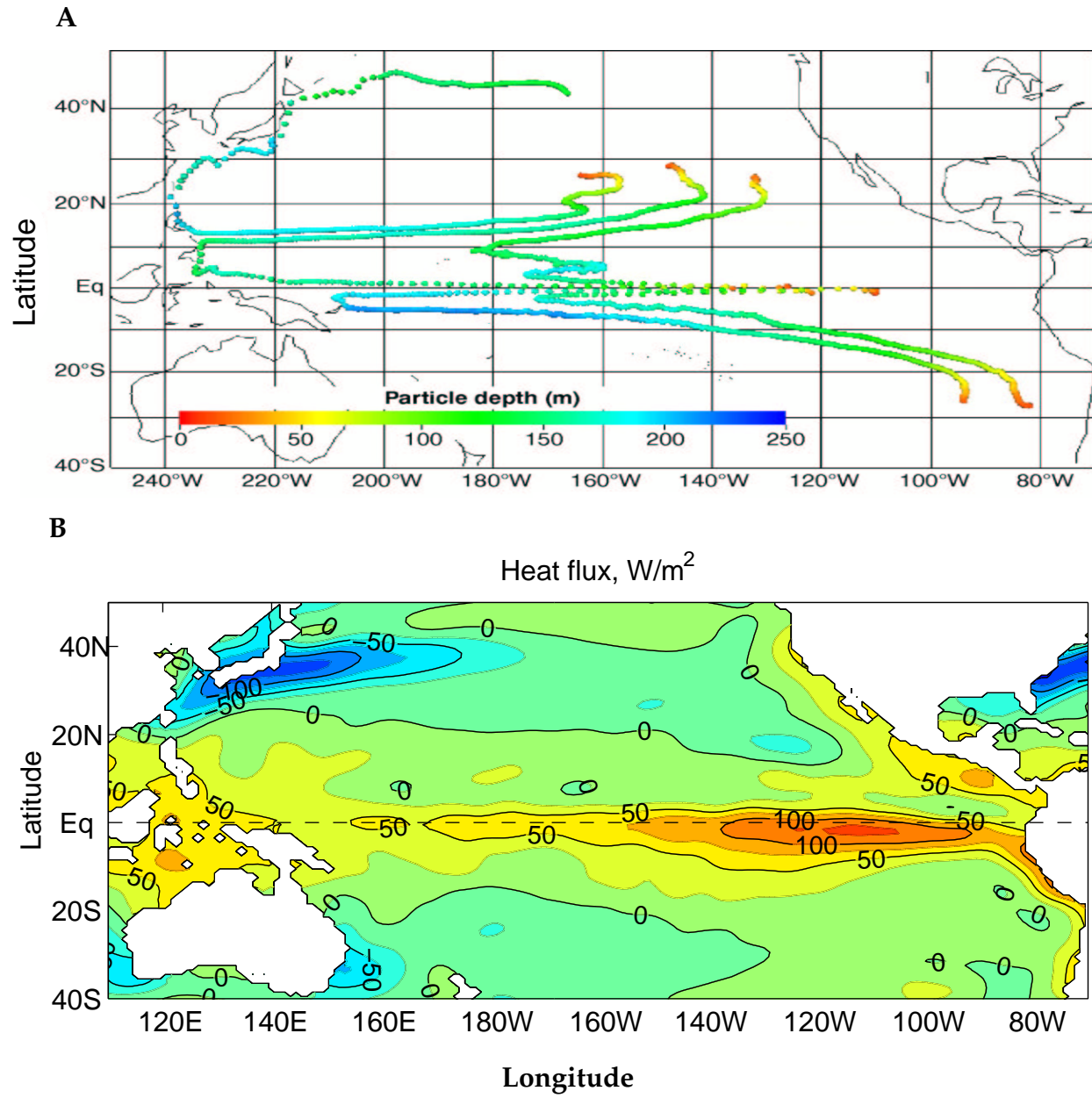


Fig 1.

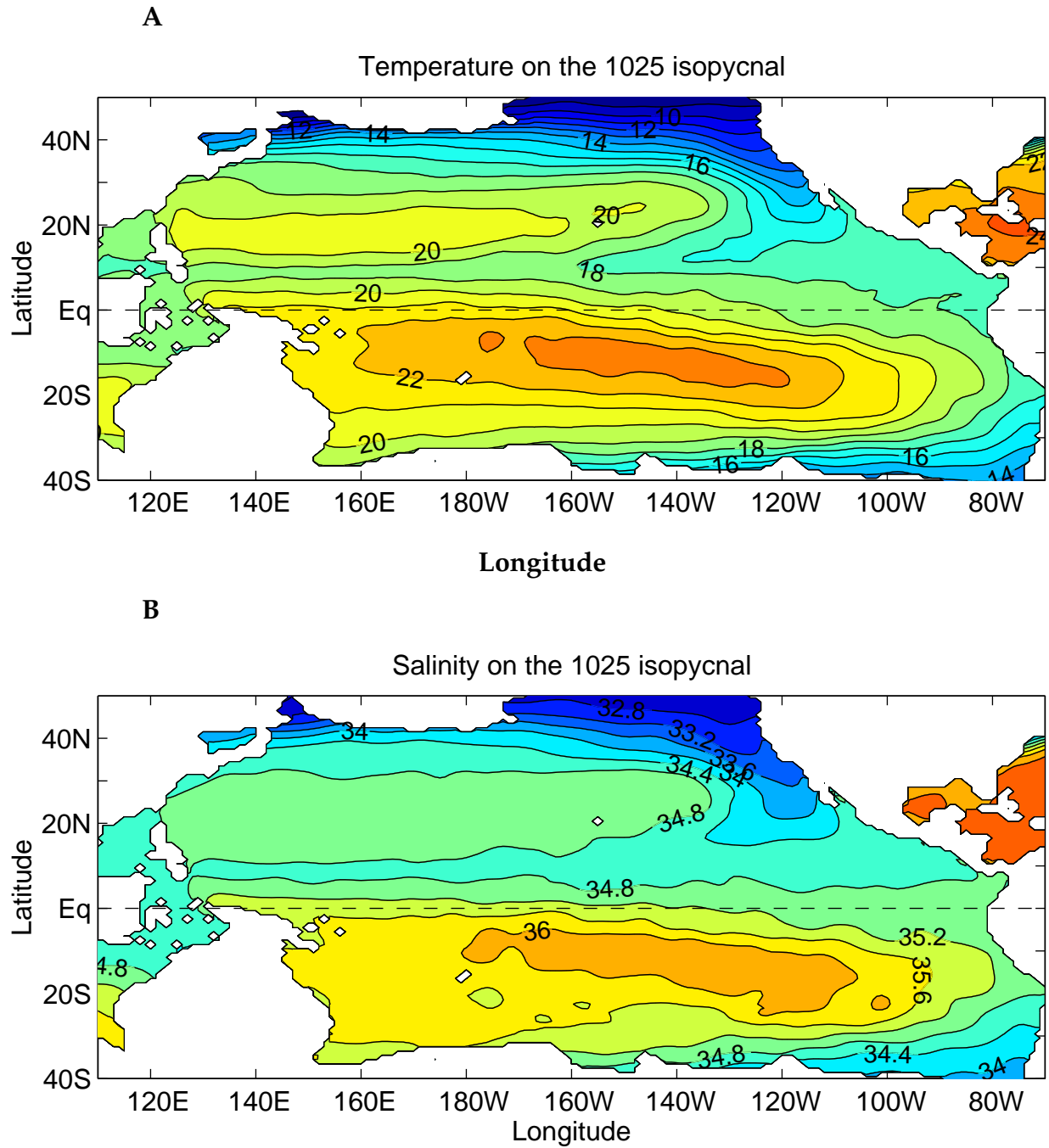


Fig 2.

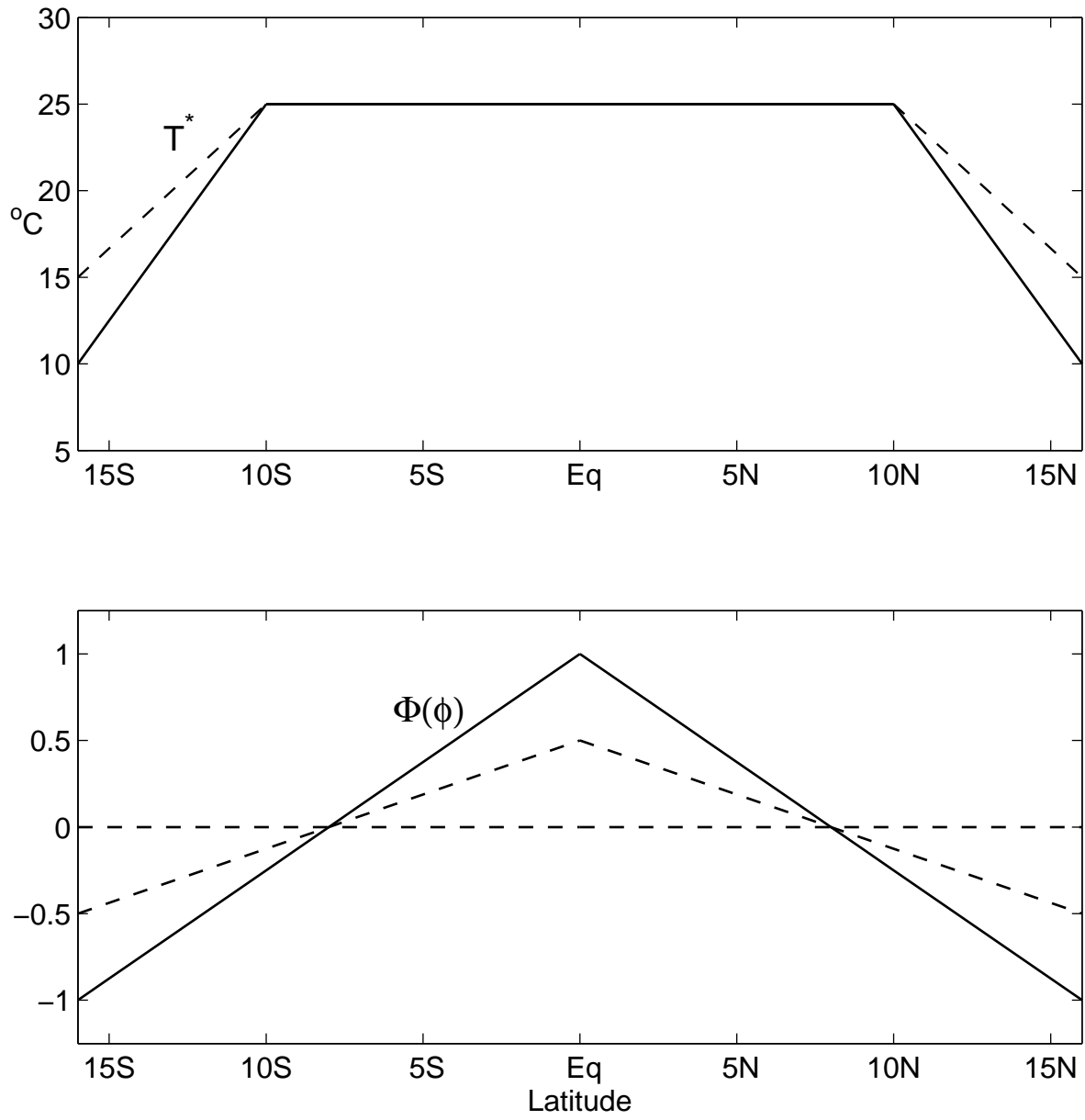


Fig. 3

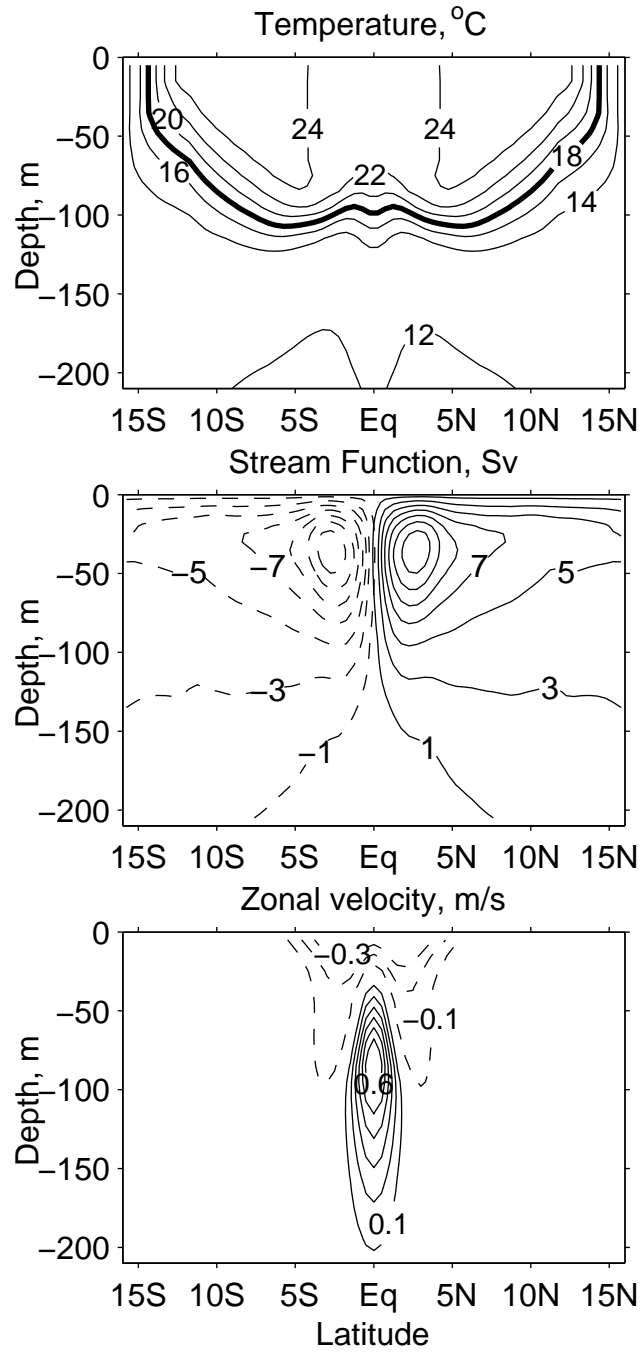


Fig. 4

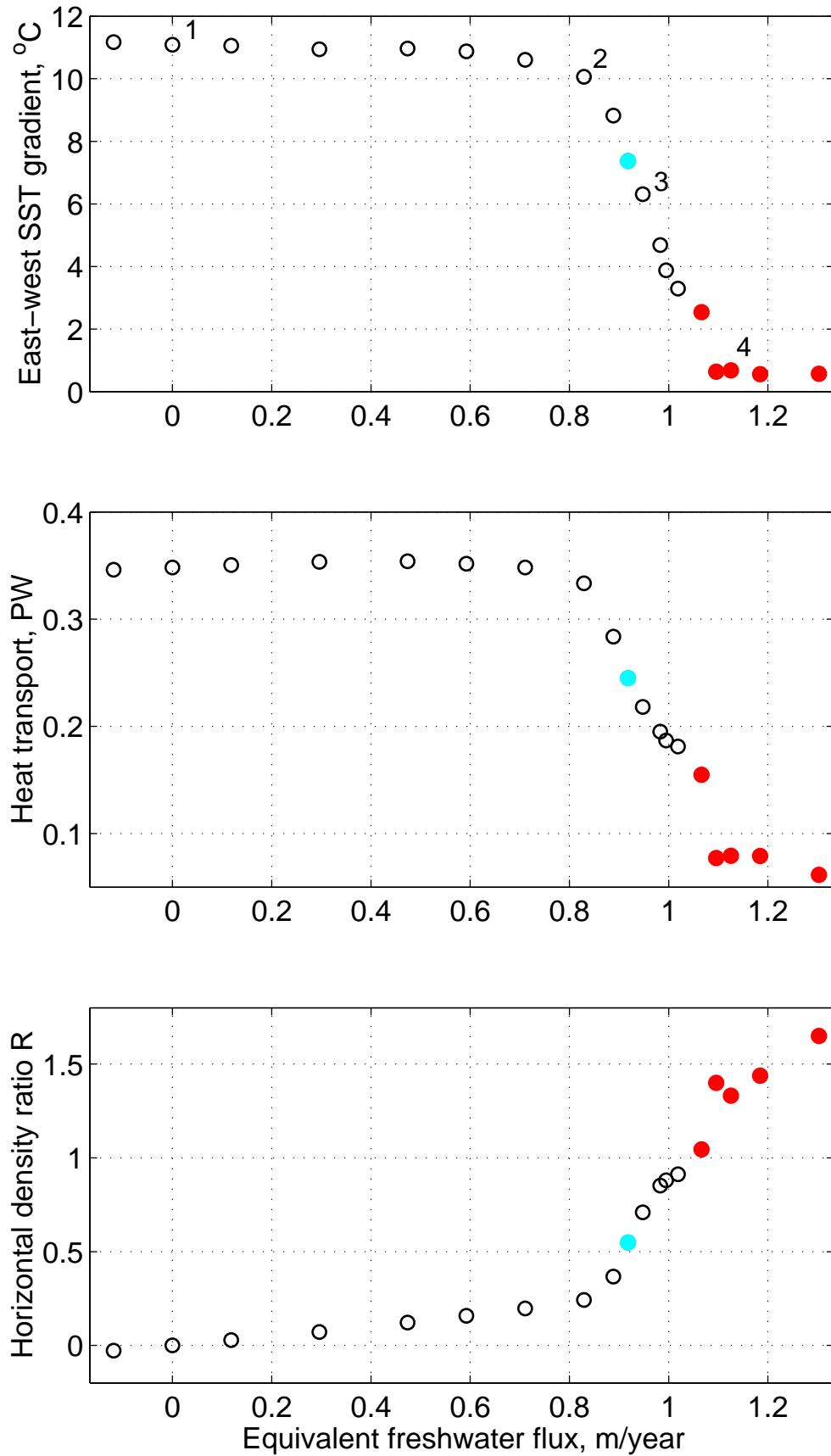


Fig. 5

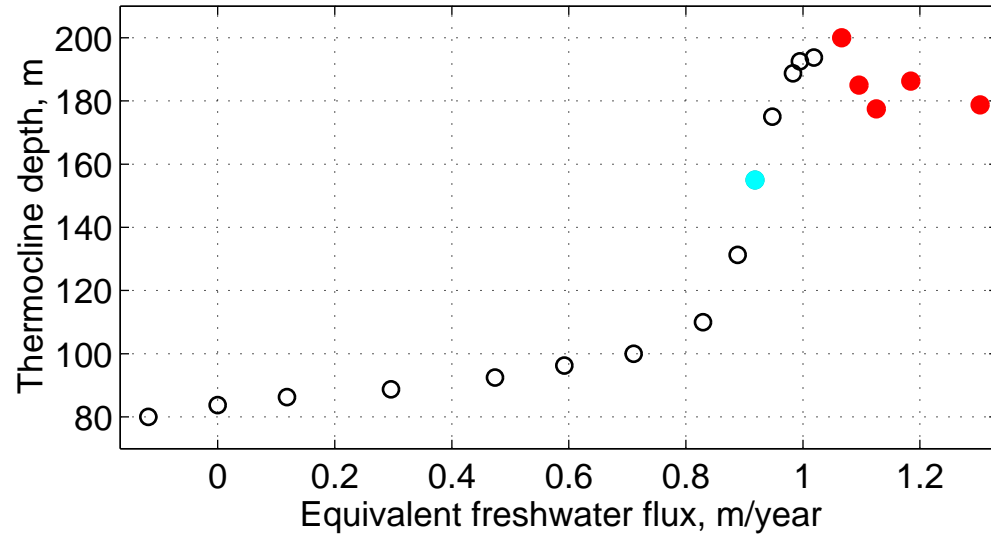


Fig. 6

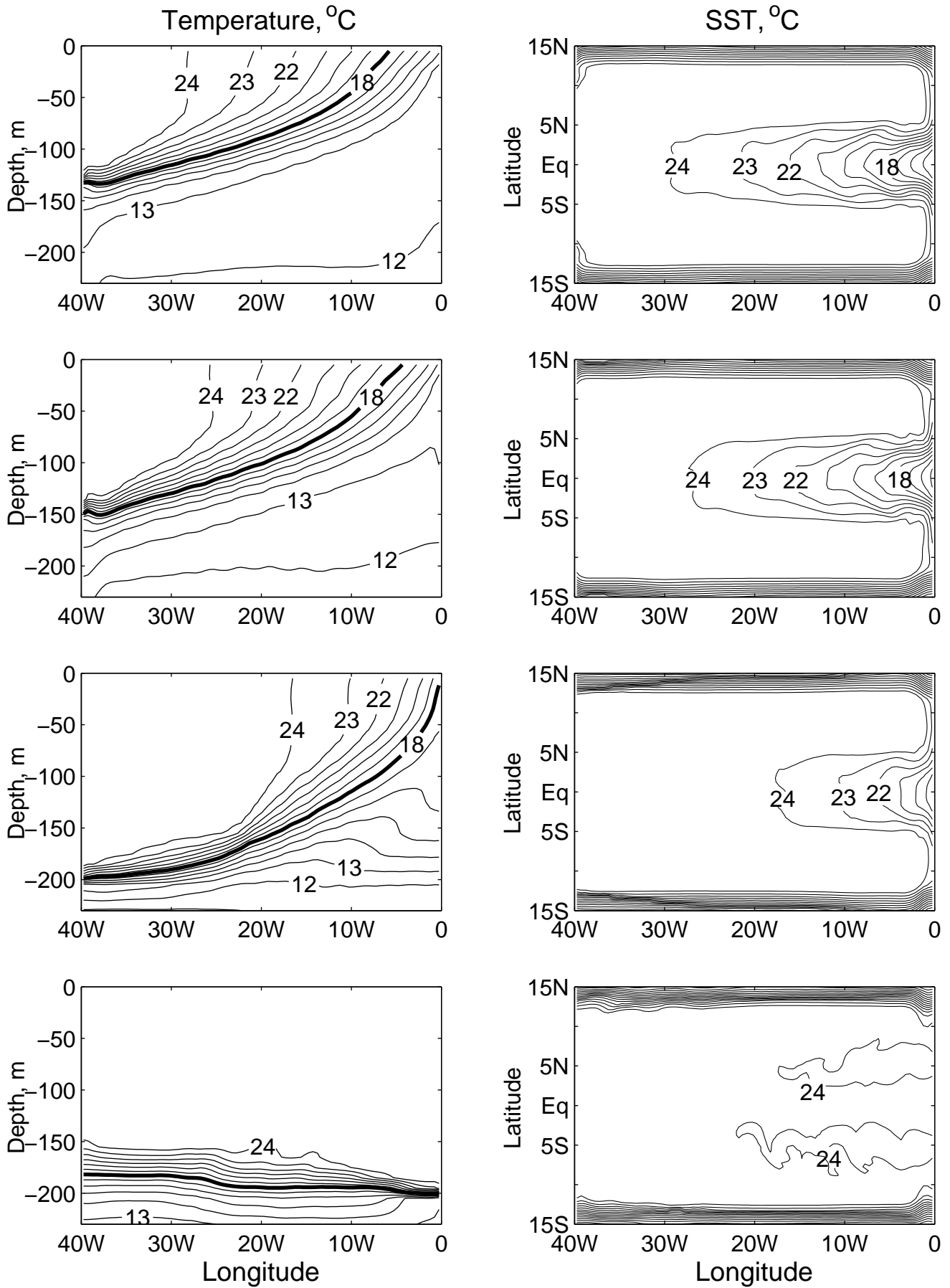


Fig. 7

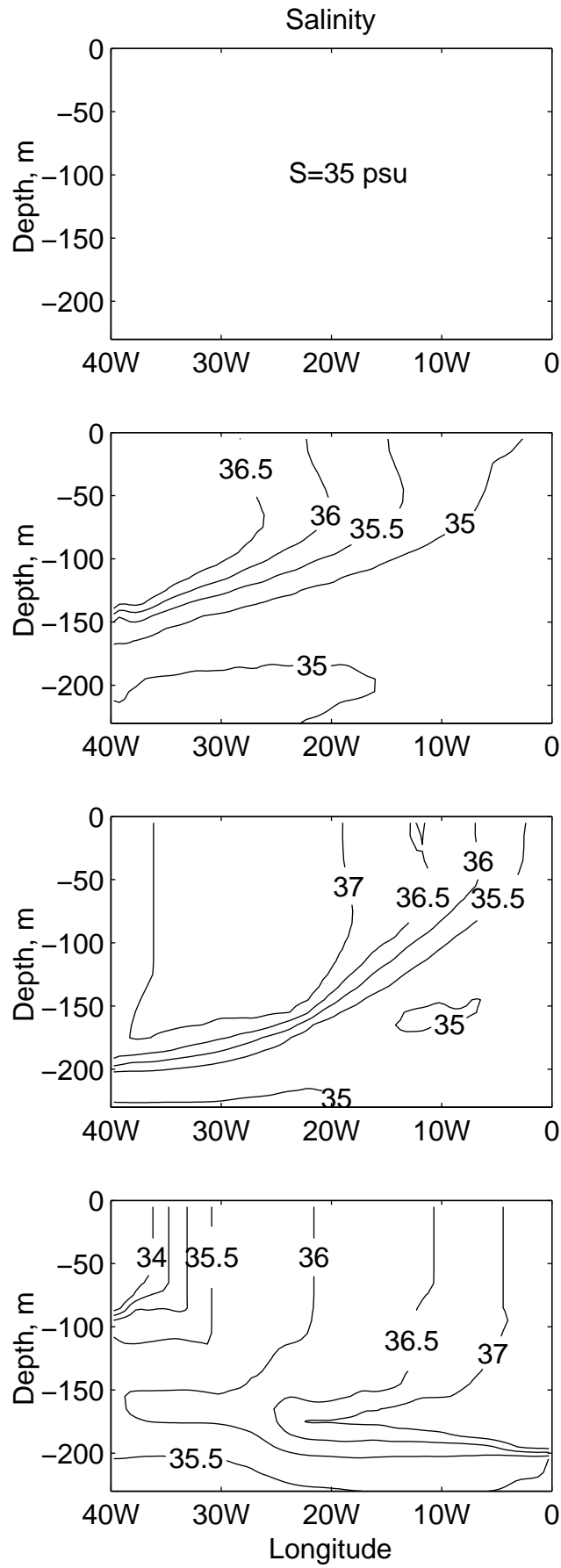


Fig. 8

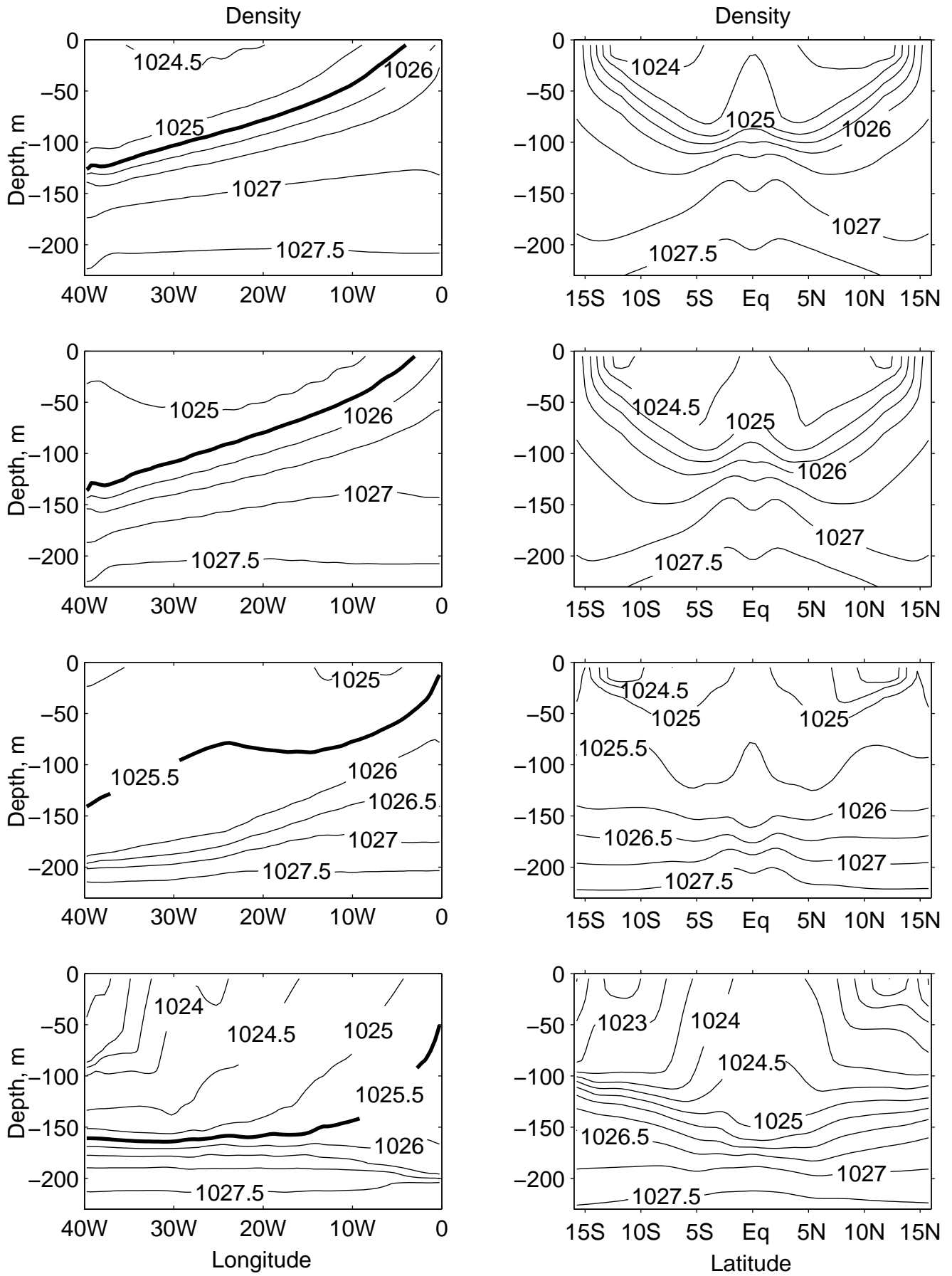


Fig. 9

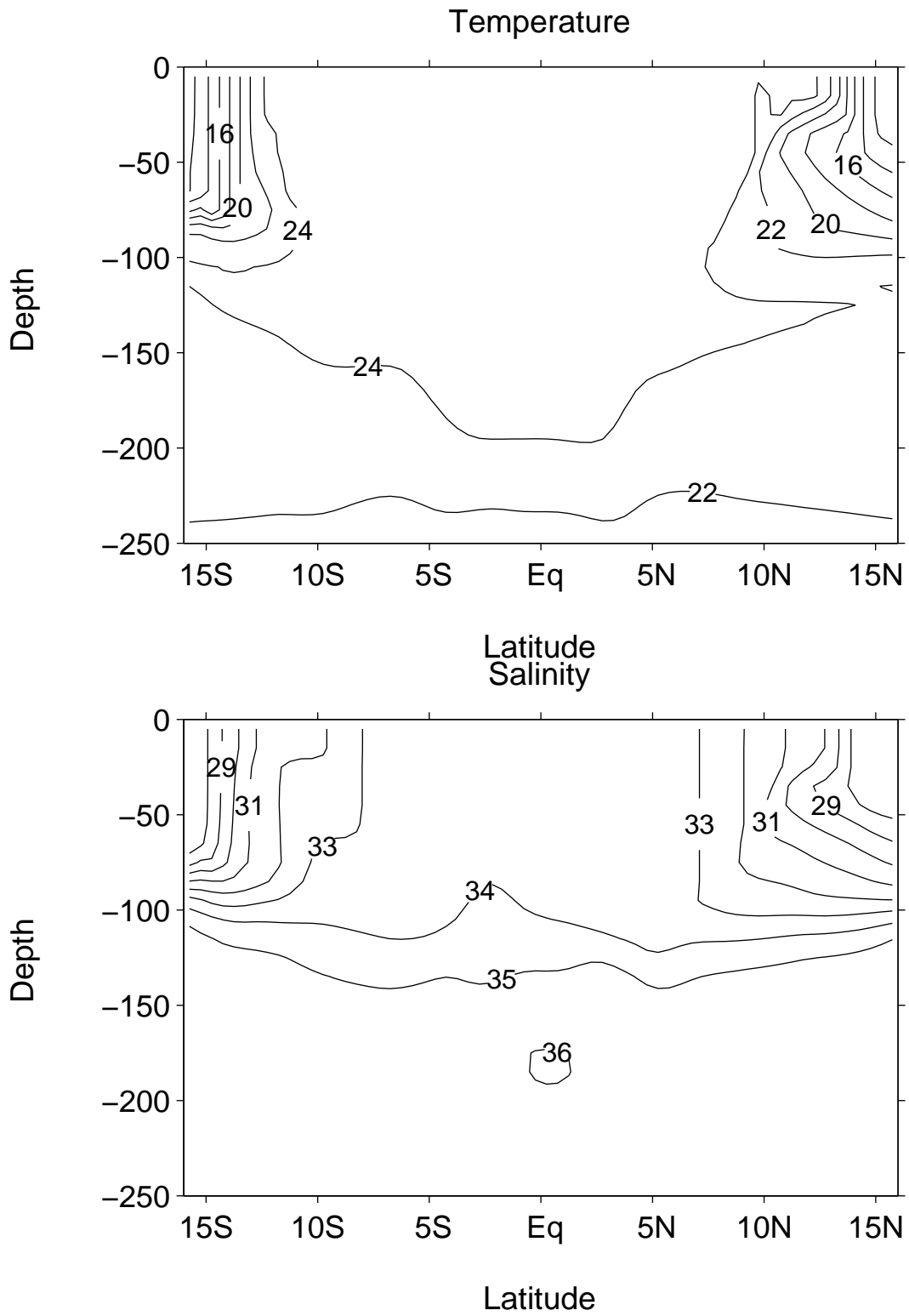


Fig. 10

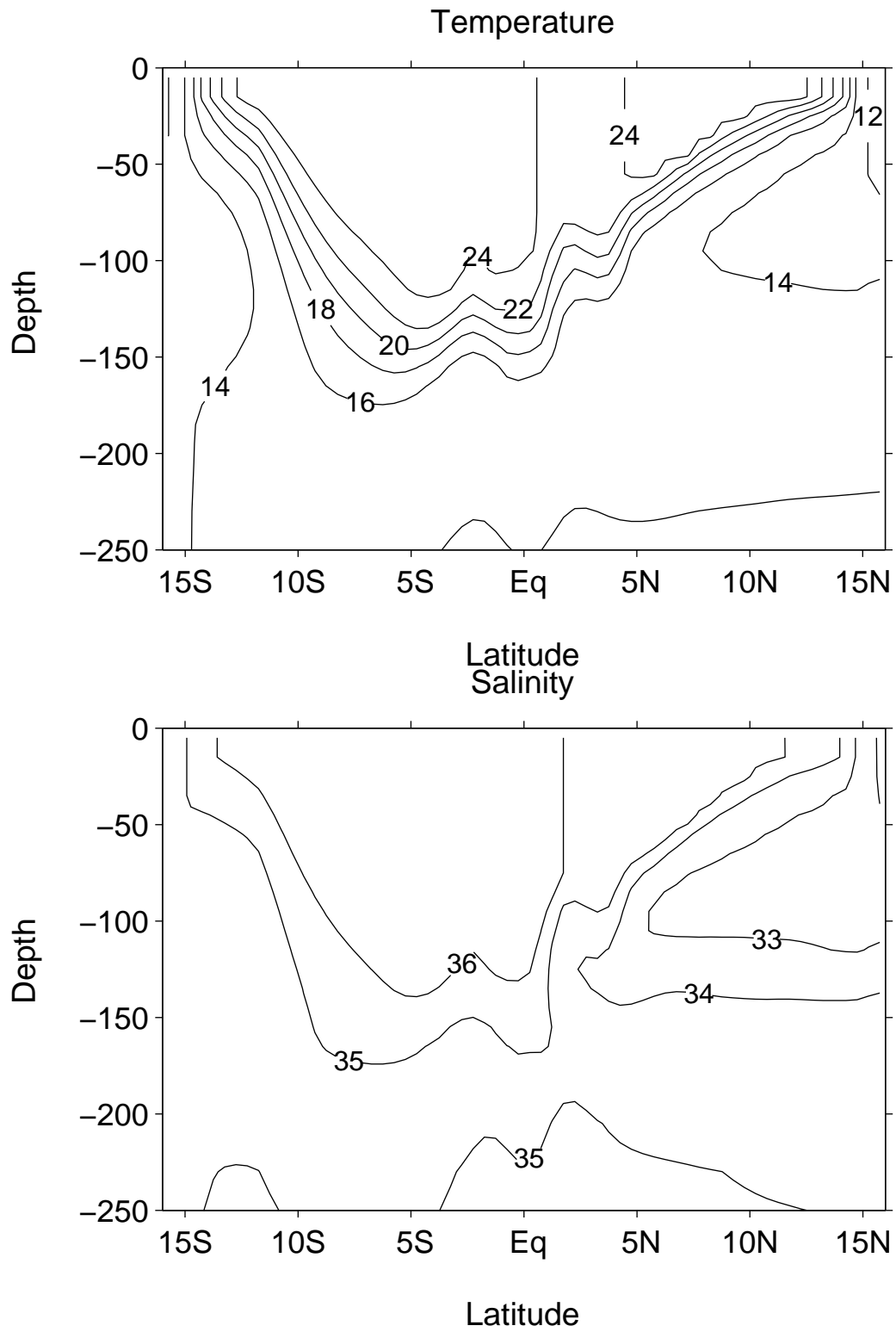


Fig. 11

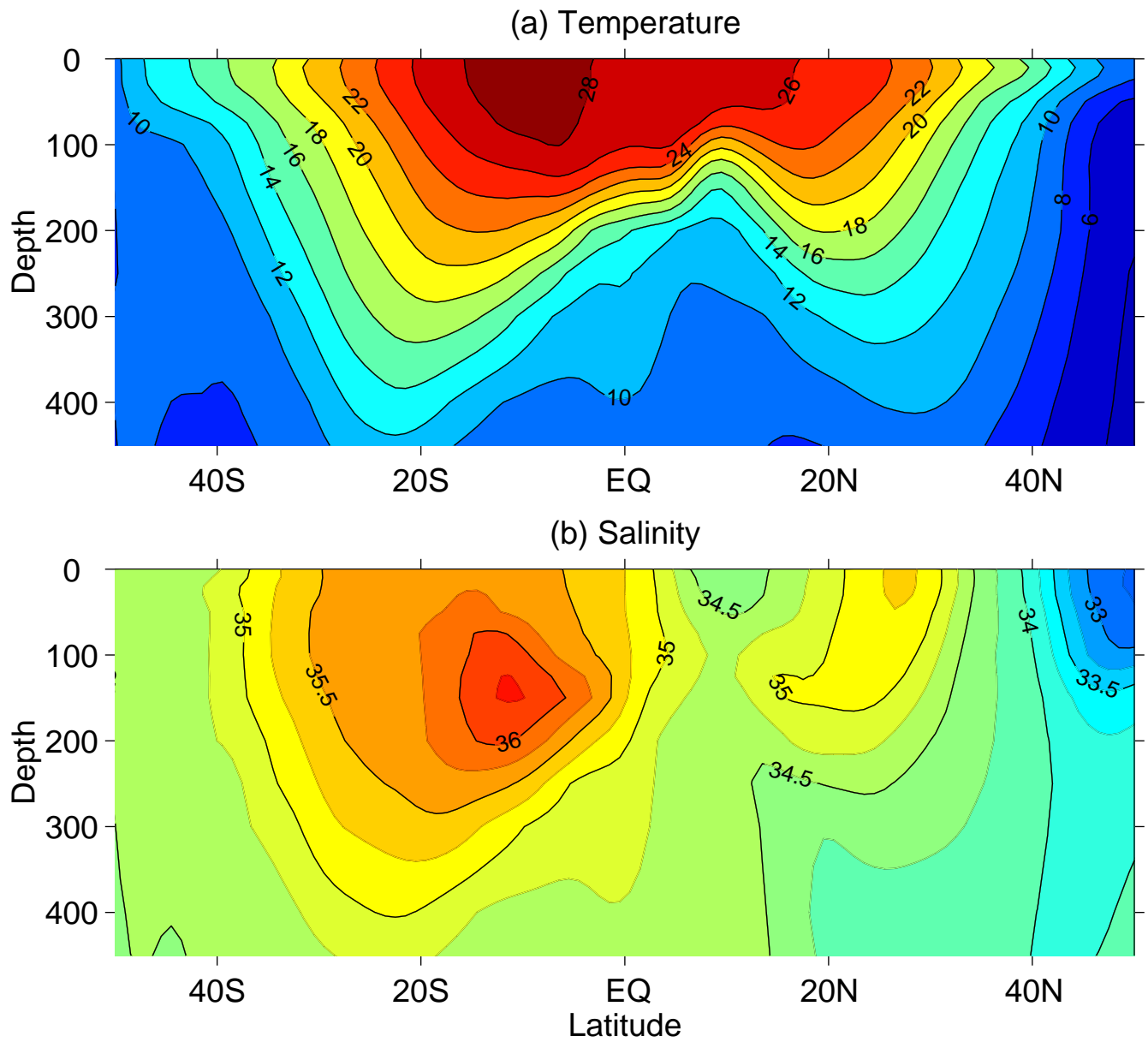


Fig. 12

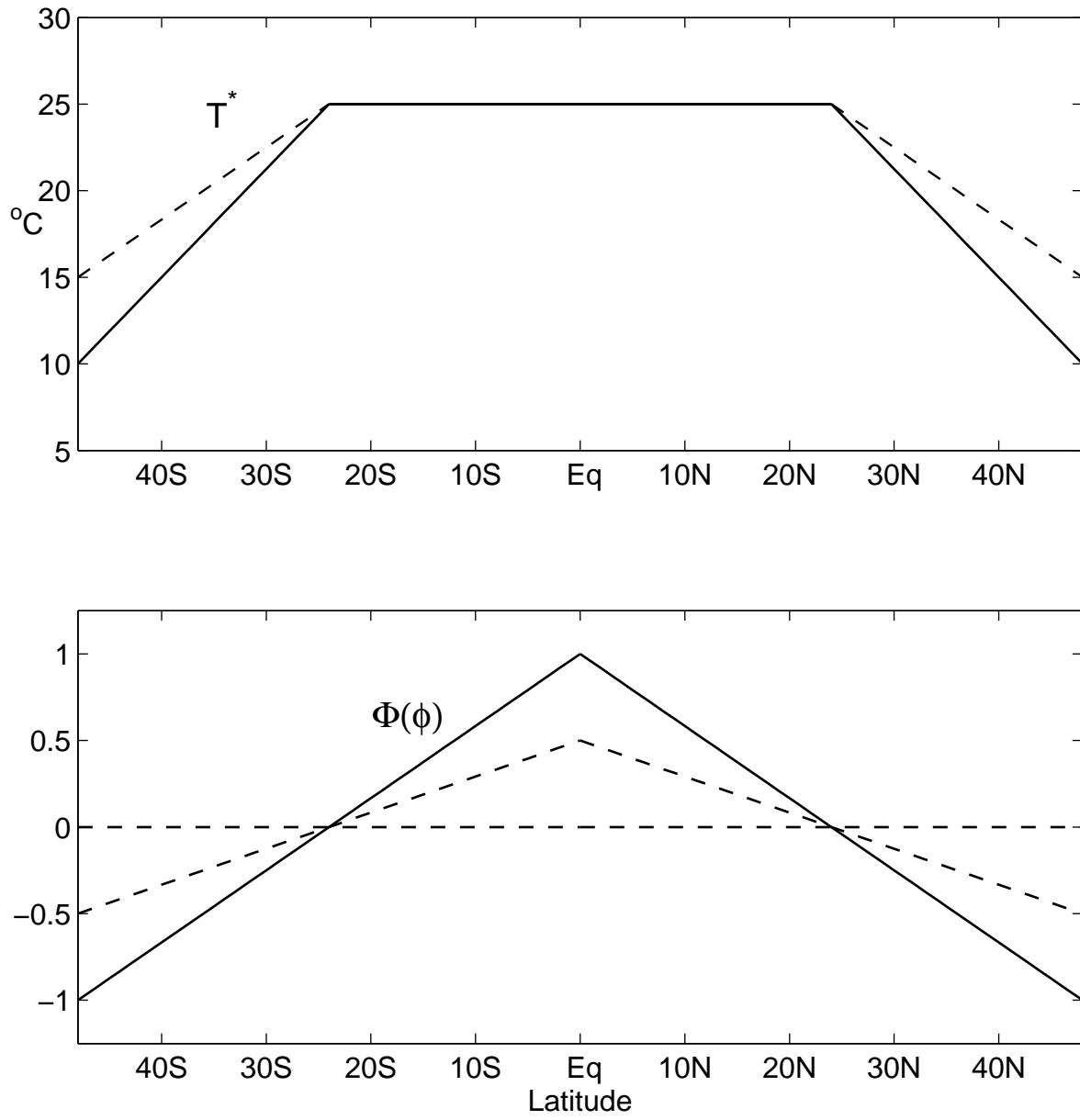


Fig. 13

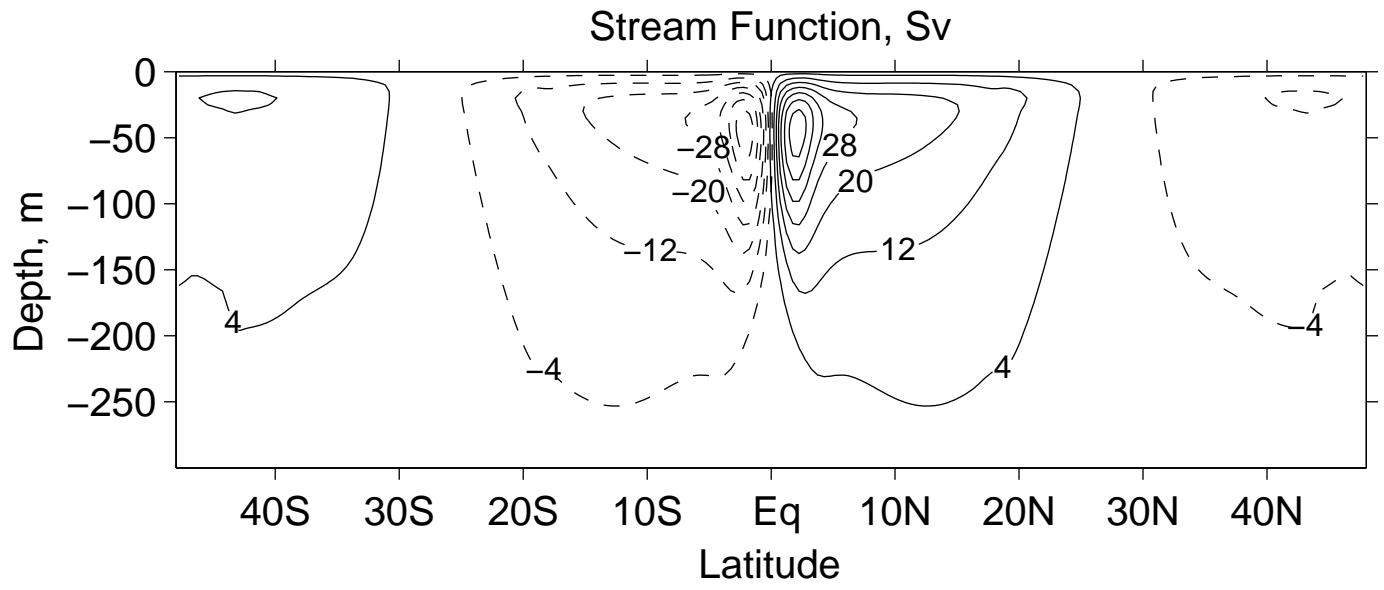


Fig. 14

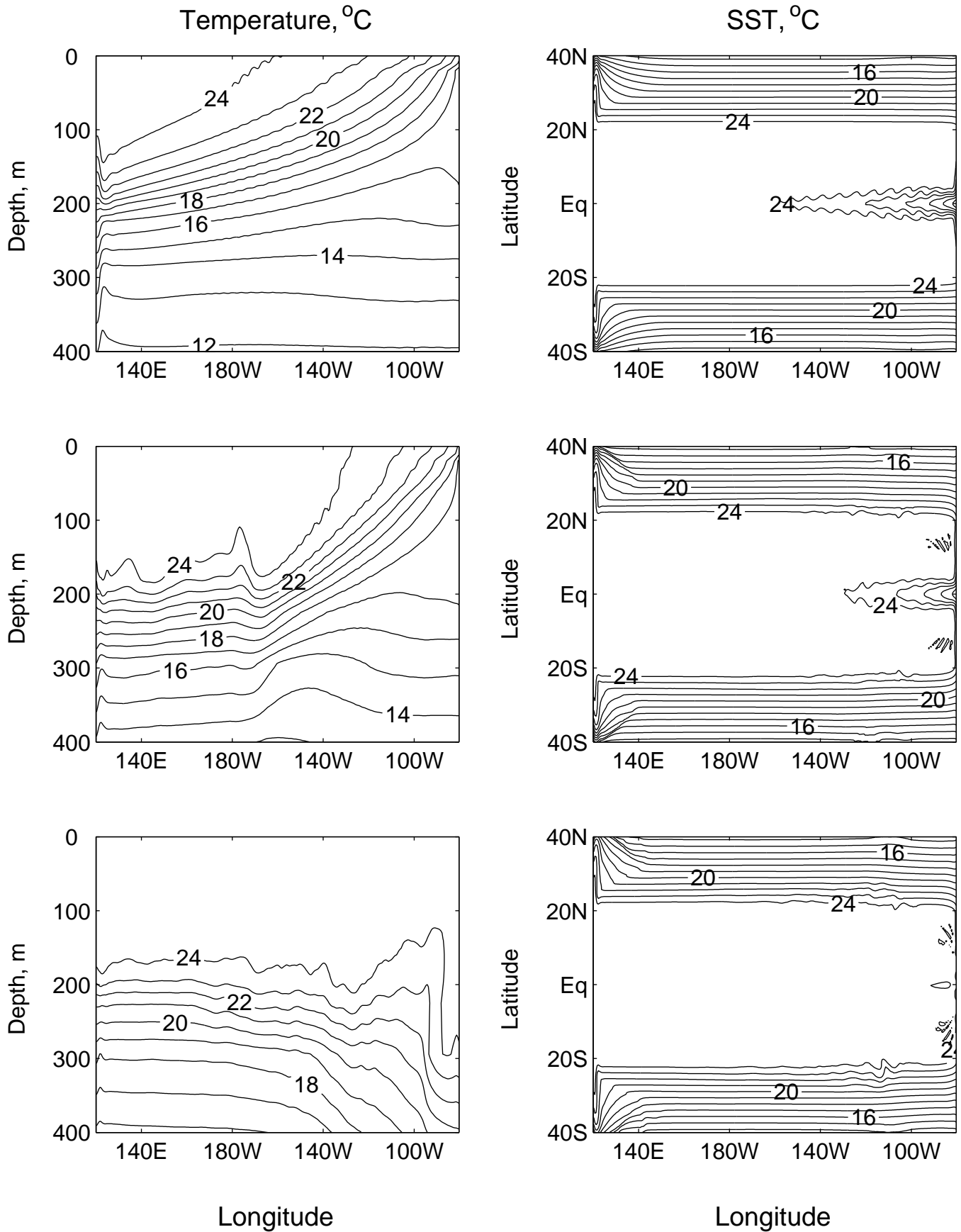


Fig .15

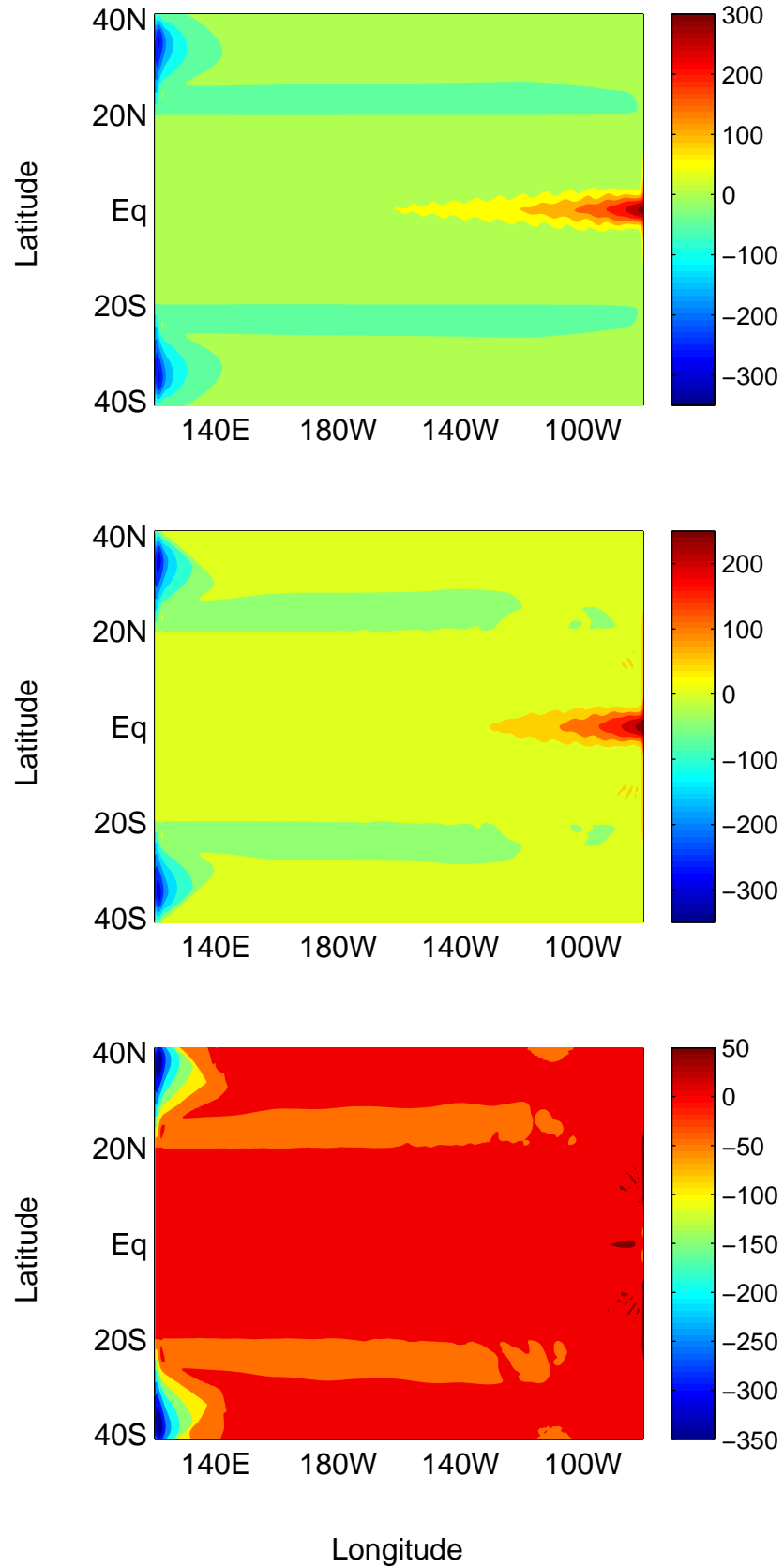


Fig. 16